ISSN 0031-918X, Physics of Metals and Metallography, 2021, Vol. 122, No. 8, pp. 775–781. © Pleiades Publishing, Ltd., 2021.
Russian Text © The Author(s), 2021, published in Fizika Metallov i Metallovedenie, 2021, Vol. 122, No. 8, pp. 831–837.

STRUCTURE, PHASE TRANSFORMATIONS, AND DIFFUSION

Stability of the Ultrafine-Grained Structure of Austenitic Corrosion-Resistant Steels during Annealing

M. V. Odnobokova[a, *], A. N. Belyakov[b], N. A. Enikeev[a], and P. O. Kaibyshev[b]

[a] *Ufa State Aviation Technical University, Ufa, 450008 Russia*
[b] *Belgorod State University, Belgorod, 308015 Russia*
**e-mail: odnobokova_marina@mail.ru*

Received December 19, 2020; revised March 2, 2021; accepted March 6, 2021

Abstract—This work focuses on the stability of the ultrafine structure in austenitic corrosion-resistant steels, such as AISI 304L (0.05 C–18.2 Cr–8.8 Ni–1.7 Mn–0.4 Si (wt %) and Fe for balance) and AISI 316L (0.04 C–17.3 Cr–10.7 Ni–1.7 Mn–0.4 Si–2 Mo (wt %) and Fe for balance) during annealing at 700°C. The ultrafine-grained structure has formed in the steels under study during rolling at 200°C due to the development of strain twinning and microshear bands. Annealing after the rolling results in continuous recrystallization and grain growth. Steel 316L has higher stability to grain growth than steel 304L, especially during annealing in the range 30–480 min. Grain growth in 316L steel during prolonged annealing is accompanied by precipitation of the Laves phase. The ultrafine-grained structure with grain size less than 1 μm is retained in 316L steel after annealing for 480 min. Grain growth during annealing is accompanied by softening of both steel grades.

Keywords: austenitic corrosion-resistant steel, rolling, ultrafine-grained structure, annealing, recrystallization, $Cr_{23}C_6$ carbide, Laves phase

DOI: 10.1134/S0031918X21070061

INTRODUCTION

Scientific and technological development requires structural materials with high strength and high ductility. Austenitic corrosion-resistant steels are currently in demand in a wide range of applications due to their high corrosion resistance in different environments. One of the effective ways to increase the mechanical strength of austenitic steels is structural strengthening through the reduction of grain size according to the Hall–Petch law [1, 2]. Severe plastic deformation or large plastic deformation at lowered temperatures is the most promising technique for structure refining in metallic materials [3]. Dislocation strengthening according to the Taylor relation can make an additional contribution to the strength as a result of such a deformation treatment [4, 5]. A low relative elongation is a common disadvantage of severely deformed metallic materials [6, 7]. The plasticity of severely deformed materials can be partially restored by subsequent annealing at a temperature at which discontinuous recrystallization is impossible. Discontinuous recrystallization is characterized by significant grain growth [8], thus preventing the retention of the ultrafine-grained structure with grains less than 1 μm in size. A favorable combination of strength and plastic characteristics was achieved during the annealing of severely deformed austenitic steels in the temperature range 700–750°C [9–11]. However, both the temperature and the annealing time influence the ultrafine-grained structure stability. Burke and Turnbull proposed a dependence describing the grain size (D) as a function of annealing time (t) in the case of collective (continuous) recrystallization or normal grain growth; i.e., $D^2 \sim K\gamma V_A t$, where K is the constant, γ is the surface energy of the boundary, and V_A is the atomic volume [12]. A change in the dislocation density (ρ) during dislocation annihilation upon annealing was described by $d\rho/dt = -C_R\rho^2$, where C_R is the constant [8]. Besides, second phases can precipitate in austenitic corrosion-resistant steels during annealing above 600°C [13], the effect of which on the grain growth resistance needs to be studied in detail. This work aims to investigate the effect of the duration of annealing at 700°C on the stability of the ultrafine-grained structure in austenitic corrosion-resistant 304L and 316L steels.

EXPERIMENTAL

For research, we used austenitic corrosion-resistant steels, such as AISI 304L (0.05 C–18.2 Cr–8.8 Ni–1.7 Mn–0.4 Si (wt %) and Fe for balance, analog of 03Kh19N10) and AISI 316L (0.04 C–17.3 Cr–10.7 Ni–1.7 Mn–0.4 Si–2 Mo (wt %) and Fe for bal-

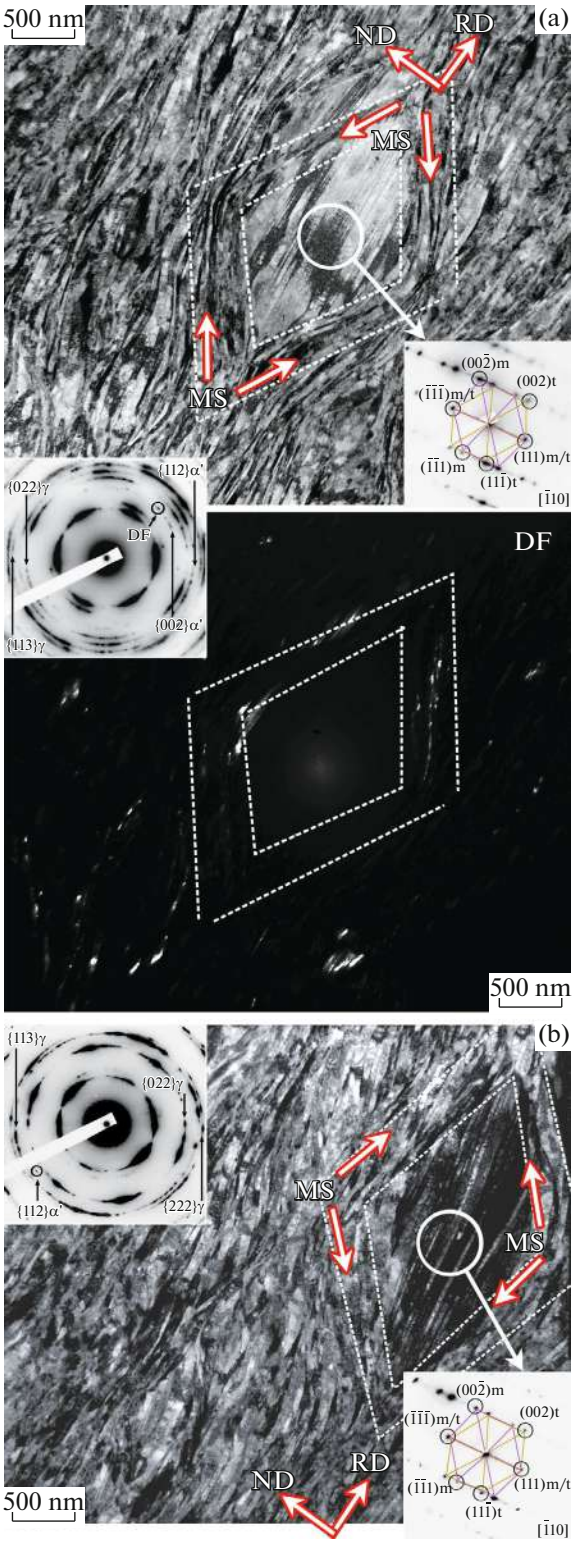

Fig. 1. Fine structure of the (a) 304L and (b) 316L steels after rolling at a temperature of 200°C to $e = 3$. Dark-field (DF) image was taken in the (022) α'-Fe reflection. MS means microshear bands, RD is the rolling direction, ND is the normal direction to the rolling plane, m is the matrix, and t means twin.

ance, analog of 03Kh17N12M2). Steel ingots were forged at 1100°C to form square billets with a cross-section of 30 × 30 mm^2. Hot forging was followed by high-temperature annealing at 1100°C for 30 min and subsequent water cooling. The initial billets formed by hot forging and high-temperature annealing were rolled into a sheet at 200°C to the true strain $e = 3$ ($e = \ln(h_0/h_k)$, where h_0 and h_k are the initial and final thickness of the steel sheet).

The rolling was followed by annealing at 700°C for 30, 60, 120, and 480 min and subsequent water cooling. Structural studies were performed using a Nova Nanosem 450 scanning electron microscope equipped with an electron backscatter diffraction (EBSD) detector and a JEOL JEM-2100 transmission electron microscope (TEM). The grain size was determined by random intercept method in the direction perpendicular to the rolling direction using EBSD maps (only high-angle boundaries (HABs) with a misorientation angle of at least 15° were taken into account). The dislocation density was determined by the number of dislocation lines visible on the foil surface using TEM. Secondary phase particles were identified by analyzing electron diffraction patterns (TEM). Flat samples with a gauge length of 16 mm and an initial cross-sectional area of 1.5 × 3 mm^2 were tested mechanically at a traverse speed of 2 mm/min using an Instron tensile machine.

RESULTS AND DISCUSSION

Figure 1 shows the fine structure of the steels after rolling at 200°C to true strain $e = 3$. Ring electron diffraction patterns indicate that the structure of the rolled steels consists of ultrafine crystallites. The crystallites are elongated along the rolling direction; therefore, they have a lamellar morphology, and their cross-sectional size is about 100–150 nm. The electron diffraction pattern of the 304L steel shows vivid {022} and {112} α'-Fe diffraction maxima. The electron diffraction pattern of the 316L steel shows only a weak {112} α'-Fe reflection. Therefore, rolling at 200°C to large plastic strains develops martensitic transformation [14]. Deformation-induced martensite crystallites are often observed in microshear bands, where they alternate with austenite crystallites (Fig. 1a, DF). The fractions of deformation-induced martensite after rolling at 200°C were about 25 and 3% in 304L and 316L steels, respectively. The fraction of deformation-induced martensite after room-temperature rolling to $e = 3$ was about 80 and 25% in 304L and 316L steels, respectively [7, 15]. In addition, heterogeneous "eye" domains can form in the structure [16], which are indicated by dotted lines in Fig. 1. According to the electron diffraction patterns, these heterogeneous regions consist of thin twins and are surrounded by microshear bands, regions with crystallites distorted by shear. The distance between the twins in the "eye" domain was about 50 nm. The orientation of the

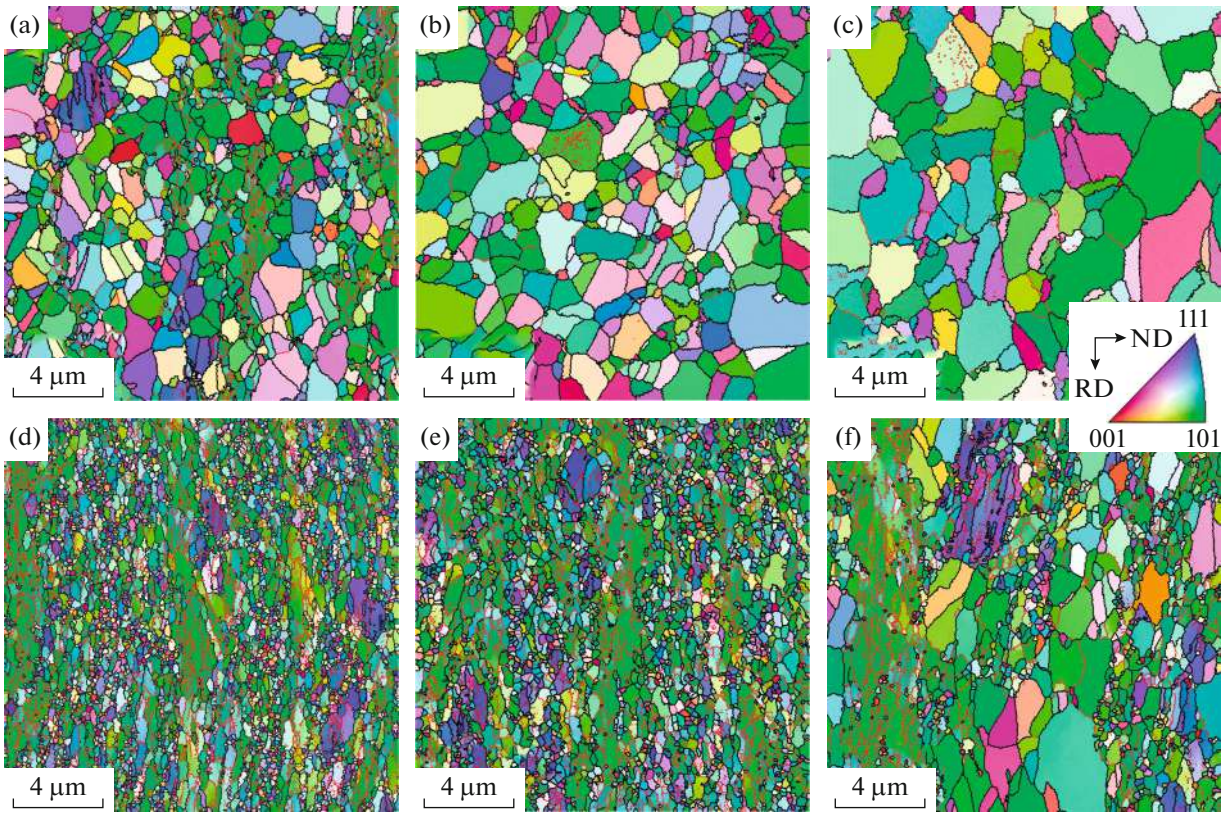

Fig. 2. Microstructure (orientational EBSD maps with the schematic boundaries) of the (a–c) 304L and (d–f) 316L steels after rolling at 200°C to $e = 3$ and subsequent annealing at 700°C for (a), (d) 30; (b), (e) 120; and (c), (f) 480 min. The normal crystallographic direction (ND) to the rolling plane is indicated by the color in the images. The black and red lines (on-line color image) correspond to high-angle and low-angle boundaries, respectively.

crystallites within the microshear bands differs from that of the crystallites inside the rest of the structure. These heterogeneous regions form due to the development of microshear bands in different directions, which leads to their intersection with each other and cutting of the twin interlayers. As a result, the twinned interlayers are surrounded by microshear bands along the four sides. The fine structure after rolling at 200°C is similar to that after room-temperature rolling, but differs in crystallite size and the fraction of deformation martensite [7, 14, 15].

Figure 2 shows the microstructure (orientational EBSD maps with the boundary schematics) of the 304L and 316L steels after rolling at 200°C to the true strain $e = 3$ and subsequent annealing at 700°C. The fine structure after annealing of the investigated 304L and 316L steels is shown in Figs. 3 and 4, respectively. Annealing of the rolled 304L and 316L steels at 700°C causes continuous recrystallization, which is more active in the 304L steel, and complete inverse $\alpha' \rightarrow \gamma$ transformation. Already 30-minute annealing results in the relatively equiaxed grain microstructure in the 304L steel, but retains the lamellar morphology of the grains in the 316L steel. A large number of deformation-induced low-angle boundaries are observed in the 316L steel microstructure. Since continuous recrystallization involves dislocation redistribution during annealing, the fine structure of the 304L steel contains 500–700 nm grains with low dislocation density in them after annealing in the time range 30–120 min (Figs. 3a–3c). The grains alternate with ultrafine crystallites. The fine structure of the 316L steel does not change significantly with increasing annealing time from 30 to 120 min and is very similar to the fine structure after rolling (Figs. 4a–4c).

The first coarse recrystallized grains appear in the 316L steel structure only after increasing the annealing time to 480 min. The higher stability of the 316L steel to continuous recrystallization and grain growth is attributed to its molybdenum alloying, as compared to the 304L steel. Molybdenum in the solid solution suppresses diffusion processes and prevents the migration of grain boundaries. Annealing for 480 min leads to the precipitation of the molybdenum-enriched Laves phase (Fe_2Mo) (Fig. 4d).

Note that $Cr_{23}C_6$ carbides precipitate in both grades of steel during annealing at 700°C (Figs. 3d, 4d, 5). The $Cr_{23}C_6$ carbides after annealing for short periods (60 min) are small in size (at most 300 nm in length, see Fig. 5), whereas they increase in size with increas-

Fig. 3. Fine structure of the 304L steel after rolling at 200°C to $e = 3$ and subsequent annealing at 700°C for (a) 30, (b) 60, (c) 120, and (d) 480 min.

ing annealing time to 480 min and can acquire a complicated morphology similar to that of (sub)grains (Fig. 4d). The $Cr_{23}C_6$ carbides precipitate simultaneously in both grades of steel, which have different stability to grain growth, indicating the lack of influence of these carbides on the migration of grain boundaries during their growth.

The presence of heterogeneous "eye" domains formed during preliminary rolling in the structure has an additional effect on the grain growth stability. The rapid growth of recrystallized grains inside these heterogeneous regions with a nanotwin structure is hindered (Fig. 5).

Figure 6 shows the effect of annealing time on the grain size and dislocation density in the 304L and 316L steels. The grain size increases gradually from 550 to 720 nm in 304L and from 300 to 400 nm in 316L when the annealing time is increased from 30 to 120 min. The grain size increases more than twofold with a subsequent increase in the annealing time to 480 min and reaches values of about 1550 and 850 nm in the 304L and 316L steels, respectively. We should note that the average grain size in the 316L steel did not exceed 1 μm after annealing at 700°C for 480 min; this means that the structure remains ultrafine-grained. The annealing time dependence of the grain size for both steels was described by $D \sim m \times t^{0.5}$ (m is a constant) [11], which was derived from the theoretical model for normal grain growth during annealing proposed by Burke and Turnbull [12]. Fitting the experimental grain size data (Fig. 6) using the above dependence yielded coefficients $m = 70$ [nm/min$^{0.5}$] for 304L steel and $m = 40$ [nm/min$^{0.5}$] for 316L steel. The value of the m coefficient is greater for the 304L steel, which is characterized by a faster grain growth kinetics.

The dislocation density in both steels decreases sharply with increasing annealing time from 30 to

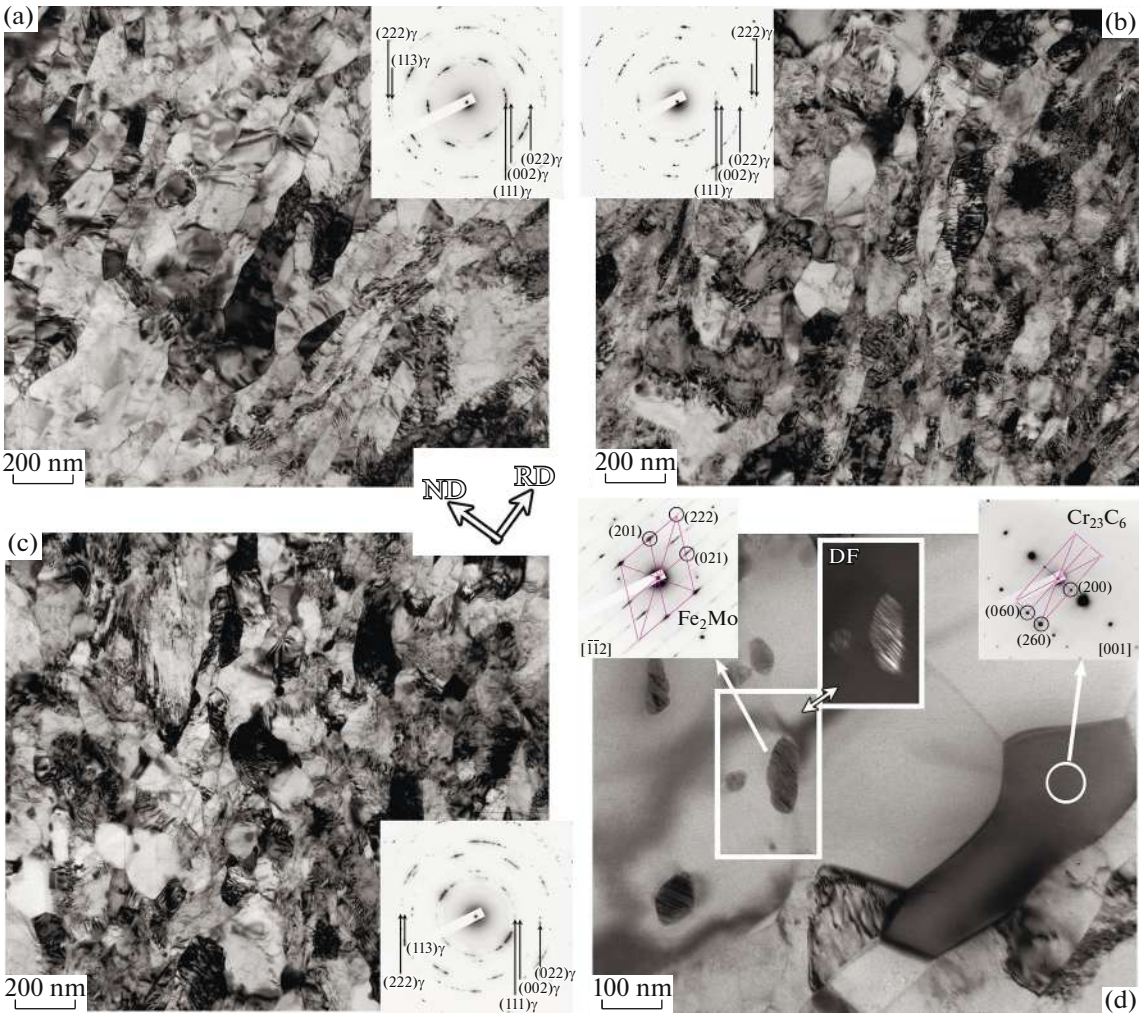

Fig. 4. Fine structure of the 316L steel after rolling at 200°C to $e = 3$ and subsequent annealing at 700°C for (a) 30, (b) 60, (c) 120, and (d) 480 min. Dark-field (DF) image was taken in the (201) Fe_2Mo reflection.

120 min (from 8 to 2×10^{14} m^{-2} in steel 304L, from 16 to 12×10^{14} m^{-2} in steel 316L), and does not change significantly with a subsequent increase in the annealing time to 480 min. The effect of the annealing time on the dislocation density was described using dependence $\rho \sim k_1 + k_2 \times t^{-1}$ (where k_1 and k_2 are constants). This dependence was derived from the model of annealing-induced dislocation annihilation, which was proposed by Humphreys and Hatherly [8], to approximate the dislocation density in Fig. 6. This approximation resulted in the following coefficient: $k_1 = 0.3$ [10^{14} m^{-2}] and $k_2 = 230$ [10^{14} m^{-2} × min] for the 304L steel, and $k_1 = 10$ [10^{14} m^{-2}] and $k_2 = 190$ [10^{14} m^{-2} × min] for the 316L steel. The k_2 coefficient for the two grades of steel has a close value, which influences the similarity of the curves. The investigated steels differ significantly in the k_1 coefficient, which is two orders of magnitude lower for the 304L steel. The curve of the dislocation density vs. annealing time for the 304L steel lies much lower than the curve for the 316L steel, which indicates the influence of the k_1 coefficient on the position of the curves.

The annealing time affects the strength of the steels under study (Fig. 7). The yield strength ($\sigma_{0.2}$) of the 304L steel gradually decreases from 770 to 580 MPa when the annealing time is increased from 30 to 480 min. The yield strength of the 316L steel does not change significantly in the annealing range 30–120 min (1030 MPa $< \sigma_{0.2} <$ 980 MPa). It decreases to 740 MPa only after annealing for 480 min.

A dependence that takes into account grain boundary and dislocation strengthening has been proposed to describe the change in the yield strength during annealing of the 316L steel [11]:

$$\sigma_{0.2} = \sigma_0 + K_y D^{-0.5} + \alpha G b \rho^{0.5}, \quad (1)$$

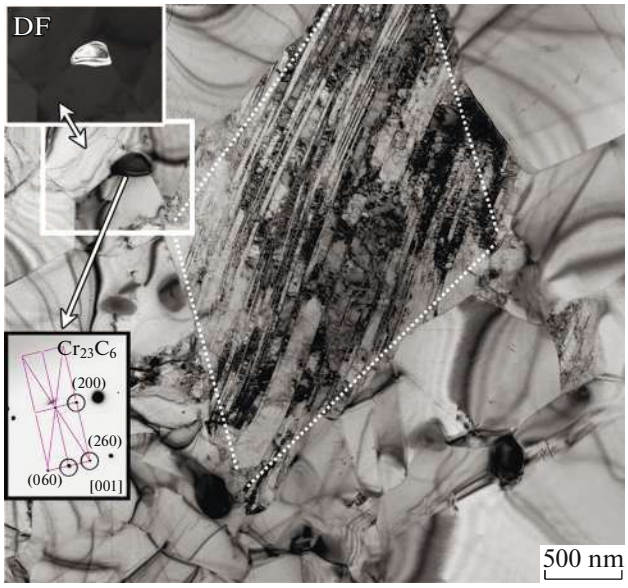

Fig. 5. Fine structure of the 304L steel after rolling at 200°C to $e = 3$ and subsequent annealing at 700°C for 60 min. Dark-field (DF) image was taken in the (200) $Cr_{23}C_6$ reflection.

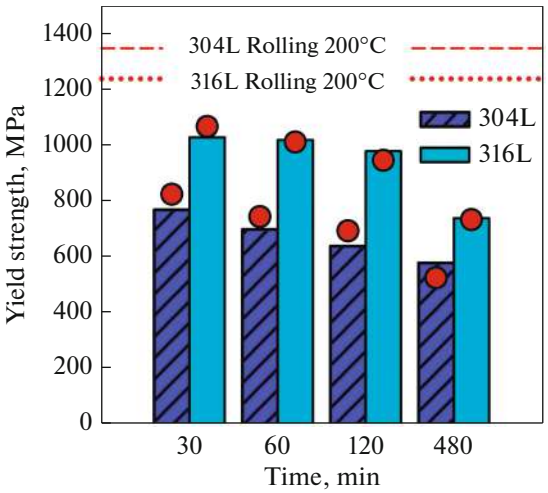

Fig. 7. Yield strength vs. time during annealing of the 304L and 316L steels at 700°C. Columns are experimental data and red dots are calculated by Eq. (1).

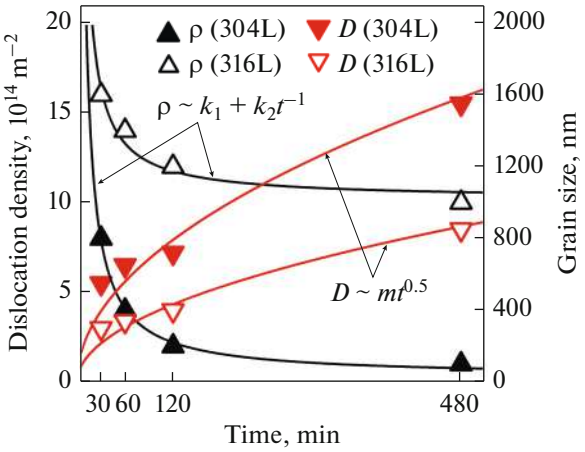

Fig. 6. Effect of the annealing time on the grain size and dislocation density in the 304L and 316L steels.

where σ_0 is the strengthening due to lattice friction, G is the shear modulus (81 000 MPa), b is the Burgers vector (0.25 nm), and K_y and α are the constants. The following coefficients $K_y = 0.4$ MPa × m$^{0.5}$ and $\alpha = 0.22$ were obtained in [11] when approximating the experimental data. The yield strengths of these steels were calculated by substituting these coefficients and $\sigma_0 = 160$ MPa [9] into Eq. (1). The calculated data are in good agreement with the experimental yield strength for the studied steels (Fig. 7). Consequently, the proposed method can be used to predict changes in the yield strength during the annealing of austenitic corrosion-resistant steels with different grain growth stability.

CONCLUSIONS

The ultrafine-grained crystalline structure with heterogeneous "eye" domains forms in the 304L and 316L steels upon rolling to $e = 3$ at 200°C. These heterogeneous regions are surrounded by microshear bands and contain nanotwins inside. These regions can be retained during subsequent annealing. Annealing of the rolled 304L and 316L steels at 700°C causes continuous recrystallization and grain growth. The 316L steel showed slower grain growth kinetics than the 304L steel. The grain size was 400 and 700 nm in the 316L and 304L steels, respectively, after annealing for 120 min. The higher stability of the ultrafine-grained structure in the 316L steel during annealing is associated with its molybdenum alloying. Molybdenum suppresses grain boundary diffusion and grain boundary migration during annealing, while molybdenum is in the solid solution. Therefore continuous recrystallization develops weakly and the grain size changes insignificantly. The Laves phase precipitates during the 480-min annealing. The precipitation of $Cr_{23}C_6$ carbides in the steel of both grades has no significant effect on the grain growth stability. The grain size and dislocation density as functions of the annealing time are described by $D \sim m \times t^{0.5}$ and $\rho \sim k_1 + k_2 \times t^{-1}$, where m, k_1, and k_2 are the constants. The yield strength of both steels can be expressed by equation $\sigma_{0.2} = \sigma_0 + K_y D^{-0.5} + \alpha G b \rho^{0.5}$, where $\sigma_0 = 160$ MPa, $K_y = 0.4$ MPa × m$^{0.5}$, and $\alpha = 0.22$.

FUNDING

This work was supported by the Russian Foundation for Basic Research (project no. 19-38-60047).

REFERENCES

1. E. O. Hall, "The deformation and ageing of mild steel: II characteristics of the Lüders deformation," Proc. Phys. Soc. B **64**, 742–747 (1951).
2. N. Petch, "The cleavage strength of polycrystals," J. Iron Steel Inst. **174**, 25–28 (1953).
3. R. Z. Valiev, R. K. Islamgaliev, and I. V. Alexandrov, "Bulk nanostructured materials from severe plastic deformation," Prog. Mater. Sci. **45**, 103–189 (2000).
4. G. I. Taylor, "The mechanism of plastic deformation of crystals. Part I. Theoretical," Proc. R. Soc. A **145**, 362–388 (1934).
5. V. V. Sagaradze and A. I. Uvarov, *Stregthening of Austenitic Steels* (Nauka, Moscow, 1989) [in Russian].
6. A. Belyakov, M. Odnobokova, A. Kipelova, K. Tsuzaki, and R. Kaibyshev, "Nanocrystalline structures and tensile properties of stainless steels processed by severe plastic deformation," IOP Conf. Series: Mater. Sci. Eng. **63**, No. 012156 (2014).
7. M. Odnobokova, A. Belyakov, and R. Kaibyshev, "Grain refinement and strengthening of austenitic stainless steels during large strain cold rolling," Philos. Mag. **99**, No. 5, 531–556 (2019).
8. F. J. Humphreys and M. Hatherly, *Recrystallization and Related Annealing Phenomena*, 2nd ed. (Elsevier, Amsterdam, 2004).
9. M. Odnobokova, A. Belyakov, N. Enikeev, D. A. Molodov, and R. Kaibyshev, "Annealing behavior of a 304L stainless steel processed by large strain cold and warm rolling," Mater. Sci. Eng., A **689**, 370–383 (2017).
10. S. Guosheng, D. Linxiu, H. Jun, Z. Bin, and R. D. K. Misra, "On the influence of deformation mechanism during cold and warm rolling on annealing behavior of a 304 stainless steel," Mater. Sci. Eng., A **746**, 341–355 (2019).
11. M. Odnobokova, Z. Yanushkevich, R. Kaibyshev, and A. Belyakov, "On the strength of a 316L-type stainless steel subjected to cold or warm rolling followed by annealing," Materials **13**, No. 2116 (2020).
12. J. Burke and D. Turnbull, "Recrystallization and grain growth," Prog. Met. Phys. **3**, 220–292 (1952).
13. B. Weiss and R. Stickler, "Phase instabilities during high temperature exposure of 316 austenitic stainless steel," Metall. Trans. **3**, 851–866 (1972).
14. M. Odnobokova, A. Belyakov, N. Enikeev, R. Kaibyshev, and R. Z. Valiev, "Microstructural changes and strengthening of austenitic stainless steels during rolling at 473 K," Metals **10**, No. 1614 (2020).
15. M. V. Odnobokova, A. N. Belyakov, I. N. Nugmanov, and R. O. Kaibyshev, "Structure and texture evolution of the metastable austenitic steel during cold working," Phys. Met. Metallogr. **121**, No. 7, 675–682 (2020).
16. H. Miura, M. Kobayashi, Y. Todaka, C. Watanabe, Y. Aoyagi, N. Sugiura, and N. Yoshinaga, "Heterogeneous nanostructure developed in heavily cold-rolled stainless steels and the specific mechanical properties," Scr. Mater. **133**, 33–36 (2017).

Translated by T. Gapontseva